Number filter for matter waves

G. Nandi,[1] A. Sizmann,[2] J. Fortágh,[3] C. Weiß,[1] and R. Walser[1]

[1]*Institut für Quantenphysik, Universität Ulm, D-89069 Ulm, Germany*
[2]*Ludwig-Maximilians-Universität München, D-80539 München, Germany*
[3]*Physikalisches Institut der Universität Tübingen, D-72076 Tübingen, Germany*

In current Bose-Einstein condensate experiments, the shot-to-shot variation of the atom number fluctuates up to 10%. In here, we present a procedure to suppress such fluctuations by using a nonlinear $p-\pi-\bar{p}$ matter wave interferometer for a Bose-Einstein condensate with two internal states and a high beam-splitter asymmetry ($p \neq 0.5$). We analyze the situation for an inhomogeneous trap within the Gross-Pitaevskii mean-field theory, as well as a quantum mechanical Josephson model, which addresses complementary aspects of the problem and agrees well otherwise.

I. INTRODUCTION

Nonlinear optical wave propagation is known to give rise to chaos, spectral and temporal distortion, or an amplification of noise [1]. This fundamentally limits the signal-to-noise ratio in state-preparation experiments or measurements. For example, nonlinearity constrains the capacity of optical communication systems [2], or the resolution of a gravitational-wave interferometer [3], where the momentum transfer to the mirror produces an intensity-dependent phase shift. However, optical nonlinearities are also capable of wave-packet self-stabilization and of a phase-sensitive reduction of noise. Second- and third-order nonlinearities, and especially the Kerr effect in optical fibers, produce energy stabilization and a noise reduction below the standard quantum limit [4–11] in various experimental configurations [12].

The past decade of matter-wave physics has also shown remarkable similarities with the development of quantum optics in the 1960s. A lucent description of this parallelism of quantum optics [13] and atomic matter waves is found in [14]. Starting from the seminal measurement of spatial coherence in normal and degenerate gases [15–18], the field has eventually progressed to study density fluctuations in trapped, three-dimensional Bose-Einstein condensates (BEC) [19–21] and fermionic gases [22]. By reducing dimensionality via geometric confinement in planar traps, one-dimensional traps, in optical lattices or on atomic chips [23], the field has now been opened to a plethora of condensed matter phenomena [24–31]. While the perfection of communication quality is the key issue for optics today, the main application for cold atomic matter waves is quantum metrology and sensing. Reaching the quantum limit and surpassing it with matter waves is a major research direction [32–42]. In this context, atoms or ions prove to be more flexible than light, as we can control many-particle entanglement and exploit different quantum statistics [43–45].

The statistical ensembles that are generated in most of the current experiments are never of the quality as theoretically envisaged. In particular, most of the current BEC experiments face a shot-to-shot variation of particle number N of about 10%. This is primarily due to technical uncertainties in the evaporation procedure [46]. If each individual BEC real-

ization would be characterized by a pure Fock state $|\psi_N\rangle$, then the uncertainty $\mathcal{P}_N$ in atom number will lead to an ensemble in a mixed state represented by a density operator

$$\rho = \sum_N \mathcal{P}_N |\psi_N\rangle\langle\psi_N|. \tag{1}$$

Thus, each observable will lose contrast caused by this number uncertainty. In this paper, we will establish an atom number filter for matter waves that allows a number stabilization, i.e., after passing each BEC through the filter the number uncertainty is less than before.

This can be achieved by using a nonlinear matter wave interferometer, cf. Figs. 1 and 3, which is in analogy to a nonlinear fiber optics setup [7]. We will assume that the condensate consists of atoms with two internal states. Due to the highly asymmetric splitting, which is crucial in this setup, the condensate fraction in one arm of the interferometer experiences a strong nonlinear phase evolution, while the other part only undergoes a weak nonlinear phase shift.

The underlying physical mechanism of the suppression of number fluctuations is based on the repulsive interaction among particles and has been used in the context of spin squeezing [47,48] or the Josephson effect [49–51]. The ideas presented here are also related to the work of Poulsen and
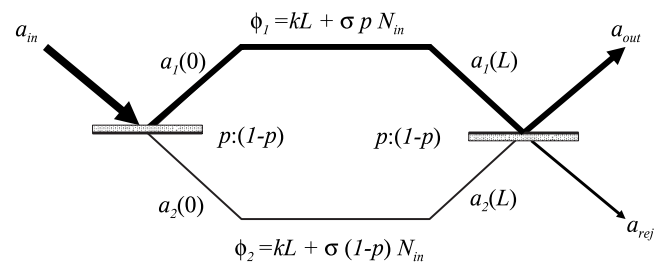
FIG. 1. Setup for an asymmetric optical nonlinear interferometer with a propagation length L and a splitting ratio $p:(1-p)$, $p \neq 0.5$. Due to a Kerr nonlinearity (susceptibility σ), one obtains a differential phase shift $\phi_{\mathrm{NL}} = \phi_1 - \phi_2 = \sigma(2p-1)N_{\mathrm{in}}$, proportional to an input photon intensity N_{in}. A subsequent self-interference of strong a_1 and weak field a_2 stabilizes the output field intensity $N_{\mathrm{out}} = |a_{\mathrm{out}}|^2$ and diverts the noise to the rejection port a_{rej}.
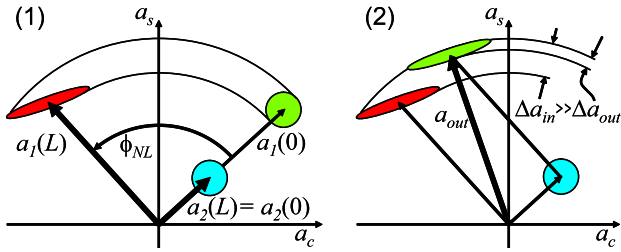
FIG. 2. (Color online) Schematic representation of the amplitude stabilization mechanism of a_{in} in an asymmetric, nonlinear interferometer in phase space with quadrature components (a_c, a_s). After the first beam splitter (1), the stronger field a_1 experiences a large nonlinear phase shift that translates amplitude fluctuations into correlated phase delay. One can neglect the nonlinear phase shift of the weaker field a_2. In a second beam splitter (2), a_2 is coherently added to the phase-shifted field a_1 to cause output in a_{out}. This stabilizes the output fluctuations well below the input level $\Delta a_{in} \gg \Delta a_{out}$, as indicated by the noise ellipses.

Mølmer [52], since their approach combines ideas for light squeezing in a nonlinear optical interferometer with the idea for spin squeezing of two spatial, initially identically occupied, condensate modes, generated via Bragg scattering. Our approach is different, as it explicitly requires a highly asymmetric splitting $p \neq 0.5$ or it would disappear at all, and it uses internal states of the atom.

This paper is organized as follows: First, we briefly review the central idea of amplitude stabilization of a nonlinear optical interferometer in Sec. II. Second, we introduce an equivalent model for a bosonic matter wave in Sec. III. This is studied within a mean-field picture to consider the effects of inhomogeneous traps as well as a Josephson model of two quantized plane wave modes, which address the quantum aspects and effects of finite particle numbers. Finally, conclusions are drawn in Sec. IV.

II. PRINCIPLE OF NONLINEAR INTERFEROMETERS IN OPTICAL FIBERS

A very fundamental type of nonlinearity, which is present in many systems, is the intensity-dependent phase shift. In photon optics it is due to the optical Kerr effect [1] characterized by a susceptibility σ and in matter waves it is caused by interatomic atom forces measured by the *s*-wave scattering length a_s. This leads to a self- or cross-phase modulation and possibly to a self-trapping potential in the nonlinear Schrödinger equation of motion of wave packets.

In the context of nonlinear interferometry [7], the intensity filtering property is best in a highly asymmetric, highly transmissive configuration, depicted in Fig. 1. The interference of a strong wave with a weak wave can eliminate a major fraction of the input noise of a_{in} in the output port a_{out}. A predominant part of the noise is channeled to the rejection port a_{rej}, consuming a small fraction of the input photon number.

Its two-step nonlinear self-stabilization mechanism is very simple and visualized in Fig. 2. After the first beam splitter, the asymmetric splitting of an input beam causes an

intensity-dependent differential phase shift between the two arms a_1 and a_2 of the interferometer. The nonlinear phase shift transforms intensity amplitude increase or reduction due to field fluctuations into a correlated phase advance or delay. Therefore, it causes a correlated phase spread relative to the average nonlinear phase shift. The second beam splitter superposes both interferometer beams coherently. It changes the quadrature angle of the field amplitude relative to the noise distribution so that the amplitude-phase correlation eliminates the amplitude noise to a large degree. For perfect stabilization, the phase advance or delay of the stronger mode relative to the weaker, quasistationary, linearly propagating mode reduces or increases the output transmission by the right amount to eliminate the input intensity fluctuations.

It has been shown that the stabilization mechanism does not only eliminate classical noise or work only with continuous-wave coherent light. Instead, this method is also applicable with broadband ultrashort solitons and in the quantum regime of field fluctuations. The fiber-optic asymmetric Sagnac interferometer has been used as a photon number filter for optical solitons [7,10]. Some of the best squeezing results have been obtained with this setup, which did not require any active stabilization. The quantum noise reduction below the shot-noise (Poisson) limit has been modeled by the quantum nonlinear Schrödinger equation (NLSE). It is in perfect agreement within the measurement uncertainty and stability has been obtained. Again, the noise reduction mechanism can be readily understood by modeling the essentials of the asymmetric interferometer by linearized fluctuations in a semiclassical approach where now the uncorrelated vacuum fluctuations are entering through the unused input port of the interferometer and where the associated phase is the soliton envelope phase. The corresponding semiclassical picture is then well represented by Fig. 2, where the noise ellipses are then the minimum uncertainty regions.

Thus, the question arises, how the analogy of the interference of bosonic fields can be applied to matter waves. The analogy is not trivial, because the quanta of the optical field and the massive bosons of the matter field are described by different ensembles. Also, on a practical side, it can be asked how well the asymmetric interferometer can function as a number filter for matter waves.

III. MODELING A NONLINEAR INTERFEROMETER WITH BOSONIC MATTER WAVES

Let us consider a trapped BEC consisting of two-level atoms labeled by $\sigma = e, g$. The complete quantum states are then denoted by $|\sigma, \mathbf{k}_\sigma\rangle$ with the internal state σ and momentum component $\mathbf{k}_\sigma$. The possibly time-dependent trapping potentials for the two species are $V_\sigma(\mathbf{r}, t)$. They are identical $V_e(\mathbf{r}, t) = V_g(\mathbf{r}, t) + \Delta$ up to a detuning Δ. The two states are coupled by a classical traveling laser field $\Omega(t) e^{i\mathbf{kr}}$ with the time-dependent Rabi frequency $\Omega(t)$ and the wave vector $\mathbf{k}$. This configuration represents a Ramsey-Bordé-interferometer (see Fig. 3) in the standard setup of atom interferometry [53]. Initially, the BEC is prepared in the $|g\rangle$ state and at an instant $t = 0$, a *p* pulse creates a superposition
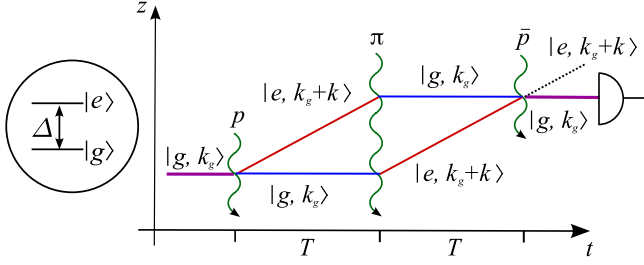
FIG. 3. (Color online) Setup for a matter-wave interferometer. Absorption of a photon k implements an asymmetric beam splitter with splitting ratio $p:(1-p)$. After a free time evolution of duration T, an optional π pulse inverts the populations. The second beam splitter with splitting ratio $\bar{p}:(1-\bar{p})$ mixes the states for the final detection of one channel and the rejection of the other (compare Fig. 1).

of $|g\rangle$ and $|e\rangle$ with a splitting ratio of the populations of $p:(1-p)$. After a time delay T, a further π pulse gives rise to an inversion of the populations. After another time interval T, a final beam splitter with splitting ratio $\bar{p}:(1-\bar{p})$ mixes the populations again.

A. Theoretical description

In principle, the dynamics of this system is governed by the Schrödinger equation $i\hbar\partial_t|\psi(t)\rangle=\hat{H}(t)|\psi(t)\rangle$ for a many-particle state $|\psi(t)\rangle$ in Fock space and with the Hamiltonian

$$\hat{H}(t) = \hat{H}_{\text{sp}}(t) + \hat{V}_d(t) + \hat{V}_p, \qquad (2)$$

where

$$\hat{H}_{\text{sp}}(t) = \int d^3r \sum_{\sigma=e,g} \hat{a}^\dagger_\sigma(\mathbf{r})\left[-\frac{\hbar^2\nabla^2}{2m} + V_\sigma(\mathbf{r},t)\right]\hat{a}_\sigma(\mathbf{r}),$$

$$\hat{V}_d(t) = \int d^3r[\hbar\Omega(t)e^{i\mathbf{k}\mathbf{r}}\hat{a}^\dagger_e(\mathbf{r})\hat{a}_g(\mathbf{r}) + \text{H.c.}],$$

$$\hat{V}_p = \frac{1}{2}\int d^3r[g_{ee}\hat{a}^\dagger_e(\mathbf{r})\hat{a}^\dagger_e(\mathbf{r})\hat{a}_e(\mathbf{r})\hat{a}_e(\mathbf{r}) + g_{gg}\hat{a}^\dagger_g(\mathbf{r})\hat{a}^\dagger_g(\mathbf{r})$$
$$\times\hat{a}_g(\mathbf{r})\hat{a}_g(\mathbf{r}) + 2g_{eg}\hat{a}^\dagger_e(\mathbf{r})\hat{a}^\dagger_g(\mathbf{r})\hat{a}_g(\mathbf{r})\hat{a}_e(\mathbf{r})].$$

In there, we introduced bosonic field operators

$$[\hat{a}_\mu(\mathbf{x}),\hat{a}^\dagger_\nu(\mathbf{y})] = \delta(\mathbf{x}-\mathbf{y})\delta_{\mu\nu}, \qquad (3)$$

and interatomic coupling constants $g_{\mu\nu}=4\pi\hbar^2a_{\mu\nu}/m$ between same and different species. $a_{\mu\nu}$ is the corresponding scattering length and m is the mass of a single particle.

In order to get physical insight into this problem, we consider two simplified scenarios. On the one hand, we study the classical field approximation in Sec. III B, where operators are replaced by complex amplitudes $\hat{a}_\sigma\to\alpha_\sigma$, which yields the Gross-Pitaevskii (GP) equation. Thus, the statistical character of the operator is neglected. Furthermore, we will consider a quasi-one-dimensional, cigar-shaped configuration with tight confinement in the radial direction [30]. The radial part can then be integrated out directly, which results in

modified coupling constants $g_{\mu\nu}\to\bar{g}_{\mu\nu}$. In the following, we tacitly drop the bar. On the other hand, the operator character is accounted for in the Josephson approximation of Sec. III C. In there, we neglect spatial inhomogeneity and consider only the behavior of two plane-wave modes.

B. Classical field approximation

Within the classical field approximation, the corresponding scaled quasi-one-dimensional GP equation reads

$$i\partial_t\begin{pmatrix}\alpha_e(z,t)\\\alpha_g(z,t)\end{pmatrix} = H_{\text{GP}}(t)\begin{pmatrix}\alpha_e\\\alpha_g\end{pmatrix},$$

$$H_{\text{GP}}(t) = -\frac{1}{2}\partial_z^2 + \begin{pmatrix}V_e(z,t)+v_e & \Omega(t)e^{ikz}\\\Omega^*(t)e^{-ikz} & V_g(z,t)+v_g\end{pmatrix}, \qquad (4)$$

where the mean-field energies are $v_\mu=g_{\mu\mu}n_\mu+g_{\mu\nu}n_\nu$, with $\mu\neq\nu\in\{e,g\}$ and $n_\sigma=|\alpha_\sigma(z,t)|^2$.

In the general case of time-dependent pulses and spatially inhomogeneous traps, it is only possible to solve this equation numerically. Results of such a calculation are presented in Sec. III B 2. However, if the system size is large and time-dependent pulses happen on short times, then one can solve this simplified situation analytically and gain qualitative understanding.

1. Bulk BEC in the Raman-Nath approximation

The beam splitter is realized by a quasi-instantaneous ($\tau\ll T,1/\Delta$) p pulse in the form of a traveling laser wave with a Rabi frequency Ω. Mathematically, this is described via the unitary S matrix

$$S_p = e^{-i\theta(e^{ikz}\sigma_+ + \text{H.c.})} = \begin{pmatrix}\cos\theta & -i\sin\theta e^{ikz}\\-i\sin\theta e^{-ikz} & \cos\theta\end{pmatrix},$$

$$\sigma_+ = \begin{pmatrix}0 & 1\\0 & 0\end{pmatrix}, \quad p = \sin^2\theta, \quad \theta = \frac{\Omega\tau}{2}, \qquad (5)$$

where the scattering phase shift θ translates into a reflection and transmission coefficient p and $1-p$, respectively.

In the following, we have propagated the mean-field state with flat potentials $V_g(z,t)=0$, $V_e(z,t)=\Delta$ for a total time $2T$ in Eq. (4). The free nonlinear evolution was interrupted by the interferometer pulse sequence $p-\pi-\bar{p}$ depicted in Fig. 3. We assume that all the population n is initially in the ground-state component $\{\alpha_e(0),\alpha_g(0)\}=\{0,\sqrt{n}\,e^{ik_gz}\}$, moving with a generic momentum k_g. The general solution for the free propagation is obtained easily by making the plane-wave ansatz

$$\{\alpha_e(z,t),\alpha_g(z,t)\} = \{\alpha_e e^{i(k_ez-\phi_e)},\alpha_g e^{i(k_gz-\phi_g)}\}, \qquad (6)$$

with time-dependent phases $\phi_\sigma(t)$ and a recoil-shifted momentum $k_e=k_g+k$. We are interested in the particle density of the output channel $n_\sigma^{\text{out}}=n_\sigma(2T)=|\alpha_\sigma(2T)|^2$ of the interferometer. After some simple algebra, one finds for the transmitted channels
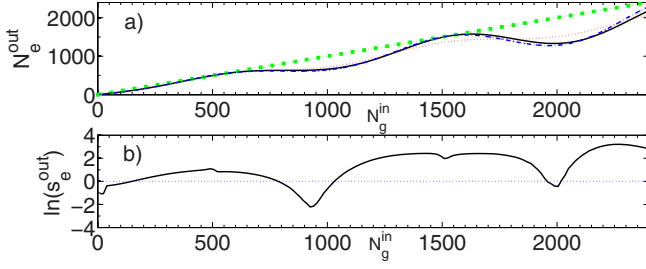
FIG. 4. (Color online) Response of a highly asymmetric $p=\bar{p}$ $=0.9$, nonlinear $p-\pi-\bar{p}$ matter-wave interferometer: (a) Mean-field result: outgoing particles in the e channel N_e^{out} vs the incoming number N_g^{in} in the g channel: homogeneous mean-field (dashed-dotted), inhomogeneous mean-field (dotted), and two-mode Josephson approximation (solid) from Eq. (20). The line marked with $\square$ is the trivial response of a $0-\pi-0$ interferometer, i.e., $N_e^{\text{out}}=N_g^{\text{in}}$ and can be used to gauge the particle loss in the unobserved channel. (b) Two-mode Josephson model: normalized number fluctuations s_e^{out} as in Eq. (21) in a semilogarithmic representation. The optimal working point for the interferometer as a number-filter device is N_g^{in} $=940$ (see Fig. 6). There, one finds a strong, sub-shot noise suppression of number fluctuations in the output channel $s_e^{\text{out}} \ll 1$.

$$n_e^{\text{out}} = n\left(\xi - \gamma \cos\left[2Tn\delta_2\left(p - \frac{1}{2}\right)\right]\right),$$

$$\xi = p\bar{p} + (1-p)(1-\bar{p}), \quad \gamma = 2\sqrt{p\bar{p}(1-p)(1-\bar{p})}, \quad (7)$$

with $\delta_2 = g_{ee} - 2g_{eg} + g_{gg}$ a central difference of scattering lengths. The population in the other channel $n_g^{\text{out}} = n - n_e^{\text{out}}$ follows from number conservation. A frequency shift of such a structure has been observed already in [54].

A simplified but less efficient form of the nonlinear interferometer is found from a symmetric mixing $\bar{p} = \frac{1}{2}$ at the final output beam-splitter

$$n_e^{\text{out}} = n\left(\frac{1}{2} - \sqrt{p(1-p)} \cos\left[2Tn\delta_2\left(p - \frac{1}{2}\right)\right]\right). \quad (8)$$

The most salient features of Eqs. (7) and (8) are the absence of linear phase shifts due to the intermediate π pulse, and the nonlinear phase shift. It is proportional to the total interaction time $2T$, to the density n, the central difference δ_2 of scattering lengths, as well as the asymmetry $p \neq 0.5$ of initial beam splitting. The oscillatory response of the interferometer with respect to a varying input particle number n stabilizes the output particle number n_e^{out}, if operated in the vicinity of a local minimum. This suppression of number fluctuations represents a nonlinear number filter for matter waves and is depicted in Fig. 4. It is also important to note that a symmetric splitting $p = \frac{1}{2}$, or vanishing central difference $\delta_2 = 0$ of scattering lengths lead to no effect at all.

Alternatively, if one considers a simplified interferometer setup in Fig. 3, i.e., without the intermediate π pulse and chooses a symmetric final beam splitting $\bar{p} = \frac{1}{2}$, one obtains

$$n_e^{\text{out}} = n\left(\frac{1}{2} + \sqrt{p(1-p)} \cos[\{\Delta_D + (\delta_1 + p\delta_2)n\}T]\right), \quad (9)$$

with a total propagation time T. This interferometer is sensitive to single particle phase shifts, here, in particular, to the Doppler-shifted detuning $\Delta_D = \Delta + k_e^2/2$ and also the difference of scattering lengths $\delta_1 = g_{eg} - g_{gg}$. For example, this setup is used for atom gravimetry [53], but it is also more susceptible to experimental noise (frequency jigger), which deteriorates visibility.

2. Weakly inhomogeneous BEC in a square well trap

In order to study the reduction of the filter performance caused by the inherent inhomogeneity of trapped atomic BECs, we have examined two scenarios. In the present section, we will consider a square-well potential

$$V_g(z,t) = \begin{cases} V_g < 0, & t < 0, \quad |z| < L \\ 0, & t \geq 0 \end{cases}, \quad (10)$$

for a confinement, while we will study a harmonically trapped system in Sec. III B 3.

After the preparation of the ground state in the trap and the first p pulse, the trap is switched off permanently. This happens identically for both trapped states, whose energy levels are detuned from the laser, i.e., $V_e(z,t) = V_g(z,t) + \Delta$. If the system length $2L$ is much larger than the healing length ζ, one can expect results that are very similar a homogeneous system of Sec. III B 1.

In the numerical simulations for the homogeneous and inhomogeneous condensates, we have used generic parameters for a quasi-1D elongated ^{87}Rb BEC with an atomic mass $m=87$ amu. In a prolate harmonic oscillator with a trapping frequency $\omega_z = 4$ s^{-1}, the basic length unit would be $a_{\text{ho}} = \sqrt{\hbar/m\omega_z} = 13.2$ μm. We have used a multiple of this scale for the length of the square-well trap $L = 132$ μm. Potential depths $V_g = -\hbar 60$ Hz and detunings $\Delta = 0$ are measured in natural energy units $\hbar\omega_z$. In a copropagating Raman laser configuration, one can have a vanishing momentum transfer $k=0$ and we assumed that the condensate is initially at rest $k_g = 0$. Short laser pulses were used such that the beam splitters were highly asymmetric $p = \bar{p} = 0.9$ and the propagation time between the pulses was $T = 20$ ms. We have deliberately modified the s-wave scattering lengths for ^{87}Rb slightly to obtain dimensionless quasi-1D coupling constants $g_{ee} = 0.034$, $g_{eg} = 0.10$, and $g_{gg} = 0.068$. Thus, the superior $p-\pi-\bar{p}$ interferometer scheme remains applicable. In principle, this can be achieved via Feshbach resonances or using other elements such as ^{85}Rb or ^{23}Na altogether.

For this situation, we have numerically solved the time-dependent inhomogeneous GP Eq. (4) and find a similar behavior as for the homogeneous limit in Fig. 4. As expected, we obtain a number stabilization of the nonlinear filter, but at a slightly reduced performance due to the inhomogeneous averaging. We have also verified that the best number stabilization is achieved for highly asymmetric splitting, and that
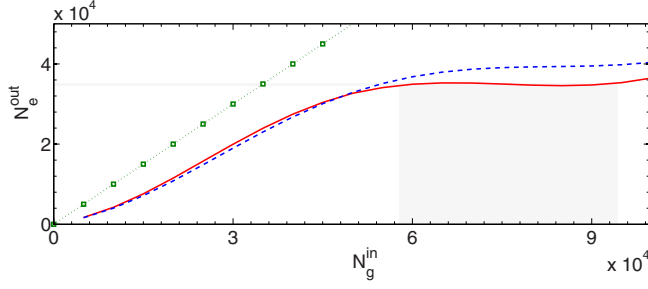
FIG. 5. (Color online) Output particle number N_e^{out} vs the input particle number N_g^{in} in a harmonically trapped, two-component BEC after passing through the interferometer. The solid (red) line represents the full numerical solution of the GP equation, while the dashed (blue) line represents $\langle N_e^{\text{out}}\rangle_{\text{TF}}$, i.e., the local density approximation of the homogeneous result Eq. (11). The gray shaded areas illustrate the compression of the number fluctuations. As in Fig. 4, the dotted line (green) marked with □ is the trivial response of a $0-\pi-0$ interferometer.

the effect does not occur for equal scattering lengths, or linear matter-wave interferometers at all.

3. Harmonically trapped BEC with a recoiless two-photon transition between hyperfine ground states

In the previous section, we have explored the number filtering properties of this interferometer primarily in quasi-homogeneous situations. However, a very common and important realization of a two-component BEC is harmonically trapped ^{87}Rb [54]. There, a two-photon microwave-rf field couples trapped hyperfine states $|g\rangle=|F=1,m_F=-1\rangle$ and $|e\rangle=|F=2,m_F=1\rangle$. Due to the low frequency of the microwave-rf fields, one can also ignore the recoil momentum imparted on the BEC.

We have studied this setup and used parameters that can be achieved experimentally by producing a cigar-shaped BEC with axial and radial trapping frequencies $\omega_z=1$ s^{-1}, $\omega_\perp=270$ s^{-1}, a beam splitter ratio of $p=0.055$, $\bar{p}=0.5$, a vanishing detuning $\Delta=0$, and quasi-1D scaled coupling parameter $g_{ee}=0.0998$, $g_{eg}=0.1036$, $g_{gg}=0.1062$. The dimensional reduction and derivation of a one-dimensional coupling parameter is achieved by a projection onto the radial ground state of the transverse oscillator [30].

It is a peculiarity of the scattering lengths of ^{87}Rb in this two-state configuration [55] that leads to a very small, yet nonvanishing value of the parameter $\delta_2=-0.0012$. But if one can achieve a reasonably long interaction time of $T=2$ s in the interferometer, one can still use the setup as a number filter. This is demonstrated in Fig. 5. Alternatively, one can turn the argument around and use this device to measure the scattering length difference δ_2 very sensitively.

To assess the validity of the numerical solution of the GP equation, we have made a simple estimate with the local density approximations (LDA). In particular, we have used the Thomas-Fermi (TF) approximation for the ground-state density $n_{\text{TF}}(z)$ in the initial harmonic oscillator mode characterized by a TF-length z_{TF} [30], which agrees well with the numerical solution as seen in Fig. 5.

$$\langle N_e^{\text{out}}\rangle_{\text{TF}} = \frac{1}{2z_{\text{TF}}}\int_{-z_{\text{TF}}}^{z_{\text{TF}}} dz\, n_{\text{TF}}(z)$$
$$\times\left\{\frac{1}{2}-\sqrt{p(1-p)}\cos\left[2Tn_{\text{TF}}(z)\delta_2\left(p-\frac{1}{2}\right)\right]\right\}. \tag{11}$$

C. Quantum mechanical two-mode approximation

In the classical field approximation for a homogeneous bulk system of Sec. III B 1, we have examined the static number filter response of the interferometer. The macroscopically occupied amplitudes were described as two coherently coupled nonlinear oscillators. They exhibited a noise suppression that is analogously used in many other physical systems ranging from electrical circuits to coupled Josephson junctions [56–58].

In order to probe the quantum aspects of such a system, we will now assume that the atomic fields $\hat{a}_\sigma(z)$ are dominated by two plane-wave modes labeled with bosonic field amplitudes $\hat{e}$ and $\hat{g}$,

$$\hat{a}_e(z) = \hat{e}e^{ik_e z} + \delta\hat{a}_e, \quad \hat{a}_g(z) = \hat{g}e^{ik_g z} + \delta\hat{a}_g. \tag{12}$$

Their residual coupling to other modes $\delta\hat{a}_\sigma$ is small at the relevant time scales and will be disregarded altogether. Within this Josephson approximation and in the quasi-1D configuration, we can simplify the Hamiltonian of Eq. (2) further to $\hat{H}\approx\hat{H}_J$ with

$$\hat{H}_J = \Delta_D\hat{n}_e + \frac{k_g^2}{2}\hat{n}_g + \Omega(t)\hat{e}^\dagger\hat{g} + \Omega^*(t)\hat{g}^\dagger\hat{e} + \frac{1}{2}g_{ee}\hat{n}_e(\hat{n}_e-1)$$
$$+ \frac{1}{2}g_{gg}\hat{n}_g(\hat{n}_g-1) + g_{eg}\hat{n}_e\hat{n}_g, \tag{13}$$

where $\hat{n}_\sigma=\{\hat{e}^\dagger\hat{e},\hat{g}^\dagger g\}$ denotes the particle number operator for the two modes and $\Delta_D=\Delta+k_e^2/2$ is the Doppler-shifted detuning as in Eq. (9). The consistency of the limit can be checked quickly by replacing the mode operators again by complex numbers, just to recover Eq. (4).

Clearly, the Josephson Hamiltonian conserves the particle number,

$$\hat{N} = \hat{n}_e + \hat{n}_g, \quad [\hat{H}_J,\hat{N}] = 0. \tag{14}$$

Thus, a general state in the N-particle sector of Fock space is given by a superposition of the states $|n_e,n_g\rangle$ with $N=n_e+n_g$,

$$|\psi_N(t)\rangle = \sum_{n=0}^{N} \psi_N^n(t)|N-n,n\rangle. \tag{15}$$

The time evolution of such a state leads to a simple one-dimensional difference equation for the time-dependent amplitudes

$$i\dot{\psi}_N^n(t) = w^n \psi_N^n + q^n(t)\psi_N^{n-1} + q^{n+1*}(t)\psi_N^{n+1}, \quad (16)$$

$$w^n = \Delta_D(N-n) + \frac{k_g^2}{2}n + \frac{1}{2}g_{gg}n(n-1)$$

$$+ \frac{1}{2}g_{ee}(N-n)(N-n-1) + g_{eg}n(N-n), \quad (17)$$

$$q^n(t) = \Omega(t)\sqrt{n(N-n+1)}, \quad (18)$$

which can be solved easily on a computer or approximated analytically [59].

From a pure quantum state $|\psi_N(t)\rangle$, one can derive expectation values of relevant observables, like the particle output in the e-channel of the interferometer $\hat{n}_e(t)$. However, the experimental reality is usually plagued with technical imperfections, day-to-day variations, or finite temperatures ensembles. Thus, one should include the possible total number uncertainty with a statistical ensemble [13] and use the time-evolved density operator $\rho(t)$, as defined in Eq. (1), to obtain observable averages. This information loss is described theoretically by a trace $\langle\ldots\rangle = \mathrm{Tr}\{\ldots\rho(t)\}$ over Fock space. In particular, this defines an output particle distribution $p(n_e, t)$ from a convolution of probabilities

$$p(n_e, t) = \langle\delta[\hat{n}_e(t) - n_e]\rangle = \sum_{N=0}^{\infty} \mathcal{P}_N |\psi_N^{N-n_e}(t)|^2, \quad (19)$$

and moments thereof in the form of expectation values, variances, and a volatility of the particle number

$$\langle\hat{n}_e(t)\rangle = \sum_{n_e=0}^{\infty} n_e p(n_e, t), \quad (20)$$

$$\sigma_e^2(t) = \langle\hat{n}_e^2(t)\rangle - \langle\hat{n}_e(t)\rangle^2, \quad s_e^{\mathrm{out}} = \frac{\sigma_e(2T)}{\langle\hat{n}_e(2T)\rangle}. \quad (21)$$

Now, we are in a position to discuss the practical aspects of the number stabilization scheme on a quantum mechanical level. First, let us consider an ideal situation where BEC's are prepared with a sharp total particle number N, such that all atoms are in the ground state $|\psi_N(t=0)\rangle = |0, n_g = N\rangle$, initially. Obviously, such a perfect laboratory has no need for an extra number filtering device and the interaction with the interferometer will even be detrimental to the number uncertainty due to the generation of shot noise. Second, if number fluctuations are present and we operate the device at the optimal working point, one should obtain a reduced number uncertainty. To illustrate this effect, we will consider a Gaussian distribution

$$\mathcal{P}_N = \mathcal{N} \exp[-(N-\bar{N})^2/2\bar{\sigma}], \quad (22)$$

which is characterized by a mean total particle number $\bar{N}$ and a width $\bar{\sigma}$.

With this uncertainty model, we have evaluated the time-dependent difference Schrödinger equation, Eq. (16), for the
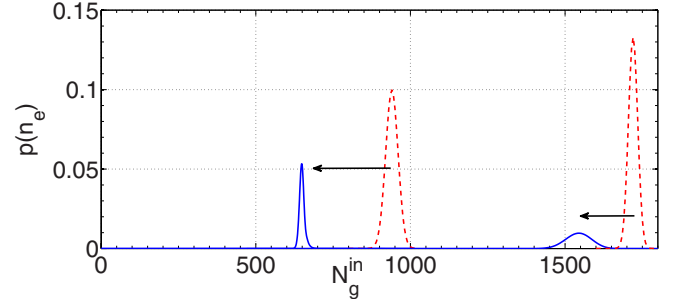
FIG. 6. (Color online) Evolution of the particle number distributions $p(n_e, 2T)$ (solid line) from two different initial distributions $\rho_{\bar{N},\bar{\sigma}}$: $(\bar{N}, \bar{\sigma}) = (940, 20)$ and $(\bar{N}, \bar{\sigma}) = (1720, 15)$ (dashed dotted line). While both distributions lose particles, the first distribution is sharpened, while the second increases its spread.

$p - \pi - \bar{p}$ interferometer for a range of initial particle numbers $0 \leq \bar{N} \leq 2500$ and two widths $\bar{\sigma} = (15, 20)$. We have also relaxed the Raman-Nath approximation for the $p - \pi - \bar{p}$ beam-splitter sequence and used extended rectangular pulses with duration $\tau = 1.31$ ms $\ll T$ and total pulse areas $\Omega\tau$ such that $p = \bar{p} = 0.9$, as before. All other parameters are as specified in Sec. III B 2.

For pure initial states $(\bar{\sigma} \to 0)$, we have depicted the results of this quantum mechanical simulation, i.e., the mean output number $\langle\hat{n}_e(2T)\rangle$ and normalized number uncertainty s_e^{out} already in Fig. 4. It can be seen that this model also agrees well with the homogeneous and inhomogeneous mean-field calculations.

Finally, we can demonstrate the number filtering by choosing two different ensembles $\rho_{\bar{N},\bar{\sigma}}$: one that corresponds to the optimal input number $(\bar{N}, \bar{\sigma}) = (940, 20)$ and one at $(\bar{N}, \bar{\sigma}) = (1720, 15)$, which leads to a further increase in the number dispersion after passing through the interferometer. In Fig. 6, we present the probability distributions $p(n_e, 2T)$ of particles leaving the e channel. The solid lines represent the final distribution and the dashed lines represent the initial distribution of particles in the g channel. The Gaussian nature of the final distribution can be understood from a semiclassical analysis of the difference equation [59]. By a further convolution with a Gaussian noise source this property remains invariant. It can be seen clearly that the first state, which is prepared at $(\bar{N}, \bar{\sigma}) = (940, 20)$, is further reduced in width despite the overall loss of the particle number, while the second state at $(\bar{N}, \bar{\sigma}) = (1720, 15)$ simply loses particles while spreading out further.

IV. CONCLUSION

In conclusion, we have analyzed the performance of a nonlinear number filter for matter waves. This addresses the problem of technical shot-to-shot variation of the particle number in current Bose-Einstein condensate experiments. A highly asymmetric $p - \pi - \bar{p}$ beam-splitter sequence is required to achieve optimal filtering performance. In the case

of symmetric splitting or the absence of nonlinearity, no filtering is seen at all. This method is in direct analogy to a nonlinear fiber optics setup studied in [6,7,10]. In detail, we have analyzed the situation for an homogeneous system and an inhomogeneous trapped gas within the Gross-Pitaevskii mean-field theory, as well as a quantum mechanical Josephson model, which addresses complementary aspects and agrees well otherwise.

[1] G. Agrawal, *Nonlinear Fiber Optics*, Third Edition (Academic Press, San Diego, 2001).

[2] P. Mitra and J. Stark, Nature (London) **411**, 1027 (2001).

[3] M. Jaekel and S. Reynaud, Europhys. Lett. **13**, 301 (1990).

[4] H. Ritze and A. Bandilla, Opt. Commun. **29**, 126 (1979).

[5] A. E. Kaplan and P. Meystre, Opt. Lett. **6**, 590 (1981).

[6] M. Kitagawa and Y. Yamamoto, Phys. Rev. A **34**, 3974 (1986).

[7] S. Schmitt, J. Ficker, M. Wolff, F. König, A. Sizmann, and G. Leuchs, Phys. Rev. Lett. **81**, 2446 (1998).

[8] M. J. Werner, Phys. Rev. Lett. **81**, 4132 (1998).

[9] N. J. Doran and D. Wood, Opt. Lett. **13**, 56 (1988).

[10] A. Sizmann and G. Leuchs, Prog. Opt. **39**, 373 (1999).

[11] D. Levandovsky, M. Vasilyev, and P. Kumar, Opt. Lett. **24**, 89 (1999).

[12] H. Bachor and T. Ralph, *A Guide to Experiments in Quantum Optics* (Wiley-VCH, Berlin, Germany, 2003).

[13] W. P. Schleich, *Quantum Optics in Phase Space* (Wiley-VCH, Berlin, Germany, 2001).

[14] K. Mølmer, New J. Phys. **5**, 55 (2003).

[15] M. Yasuda and F. Shimizu, Phys. Rev. Lett. **77**, 3090 (1996).

[16] M. Andrews, C. Townsend, H.-J. Miesner, D. Durfee, D. Kurn, and W. Ketterle, Science **275**, 637 (1997).

[17] B. Saubaméa, T. W. Hijmans, S. Kulin, E. Rasel, E. Peik, M. Leduc, and C. Cohen-Tannoudji, Phys. Rev. Lett. **79**, 3146 (1997).

[18] I. Bloch, T. Hänsch, and T. Esslinger, Nature (London) **403**, 166 (2000).

[19] C. Orzel, A. Tuchman, M. Fenselau, and M. K. M. Yasuda, Science **291**, 2386 (2001).

[20] C.-S. Chuu, F. Schreck, T. P. Meyrath, J. L. Hanssen, G. N. Price, and M. G. Raizen, Phys. Rev. Lett. **95**, 260403 (2005).

[21] M. Schellekens, R. Hoppeler, A. Perrin, J. V. Gomes, D. Boiron, A. Aspect, and C. Westbrook, Science **310**, 648 (2005).

[22] T. Jeltes, J. McNamara, W. Hogervorst, W. Vassen, V. Krachmalnicoff, M. Schellekens, A. Perrin, H. Chang, D. Boiron, A. Aspect *et al.*, Nature (London) **445**, 402 (2007).

[23] J. Fortágh and C. Zimmermann, Rev. Mod. Phys. **79**, 235 (2007), and references therein.

[24] D. Jaksch, C. Bruder, J. I. Cirac, C. W. Gardiner, and P. Zoller, Phys. Rev. Lett. **81**, 3108 (1998).

[25] A. Görlitz, J. M. Vogels, A. E. Leanhardt, C. Raman, T. L. Gustavson, J. R. Abo-Shaeer, A. P. Chikkatur, S. Gupta, S. Inouye, T. Rosenband, and W. Ketterle, Phys. Rev. Lett. **87**, 130402 (2001).

[26] M. Greiner, O. Mandel, T. Esslinger, T. Hänsch, and I. Bloch, Nature (London) **415**, 39 (2002).

[27] T. Stöferle, H. Moritz, C. Schori, M. Köhl, and T. Esslinger, Phys. Rev. Lett. **92**, 130403 (2004).

[28] I. Bloch, Nat. Phys. **1**, 23 (2005).

[29] D. Hellweg, L. Cacciapuoti, M. Kottke, T. Schulte, K. Sengstock, W. Ertmer, and J. J. Arlt, Phys. Rev. Lett. **91**, 010406 (2003).

[30] R. Walser, Opt. Commun. **243**, 107 (2004).

[31] T. Kinoshita, T. Wenger, and D. S. Weiss, Phys. Rev. Lett. **95**, 190406 (2005).

[32] N. Ramsey, Rev. Mod. Phys. **62**, 541 (1990).

[33] M. Kitagawa and M. Ueda, Phys. Rev. Lett. **67**, 1852 (1991).

[34] M. J. Holland and K. Burnett, Phys. Rev. Lett. **71**, 1355 (1993).

[35] D. J. Wineland, J. J. Bollinger, W. M. Itano, and D. J. Heinzen, Phys. Rev. A **50**, 67 (1994).

[36] P. Berman, *Atom Interferometry* (Academic Press, San Diego, 1997).

[37] A. Vogel, M. Schmidt, K. Sengstock, K. Bongs, W. Lewoczko, T. Schuldt, A. Peters, T. V. Zoest, W. Ertmer, E. Rasel *et al.*, Appl. Phys. B: Lasers Opt. **84**, 663 (2006).

[38] G. Nandi, R. Walser, E. Kajari, and W. P. Schleich, Phys. Rev. A **76**, 063617 (2007).

[39] E. Kajari, R. Walser, W. Schleich, and A. Delgado, Gen. Relativ. Gravit. **36**, 2289 (2004).

[40] K. Eckert, P. Hyllus, D. Bruss, U. V. Poulsen, M. Lewenstein, C. Jentsch, T. Müller, E. M. Rasel, and W. Ertmer, Phys. Rev. A **73**, 013814 (2006).

[41] S. Dimopoulos, P. W. Graham, J. M. Hogan, and M. A. Kasevich, Phys. Rev. Lett. **98**, 111102 (2007).

[42] W. Li, A. Tuchman, H.-C. Chien, and M. Kasevich, Phys. Rev. Lett. **98**, 040402 (2007).

[43] K. Mølmer and A. Sørensen, Phys. Rev. Lett. **82**, 1835 (1999).

[44] B. Julsgaard, A. Kozhekin, and E. Polzik, Nature (London) **413**, 400 (2001).

[45] A. Sørensen, L.-M. Duan, J. I. Cirac, and P. Zoller, Nature (London) **409**, 63 (2001).

[46] M. Köhl, M. J. Davis, C. W. Gardiner, T. W. Hänsch, and T. Esslinger, Phys. Rev. Lett. **88**, 080402 (2002).

[47] M. Kitagawa and M. Ueda, Phys. Rev. A **47**, 5138 (1993).

[48] L. You, Phys. Rev. Lett. **90**, 030402 (2003).

[49] J. Javanainen and M. Y. Ivanov, Phys. Rev. A **60**, 2351 (1999).

[50] A. Leggett, Rev. Mod. Phys. **73**, 307 (2001).

[51] R. Gati, J. Esteve, B. Hemmerling, T. Ottenstein, J. Appmeier, A. Weller, and M. Oberthaler, New J. Phys. **8**, 189 (2006).

[52] U. V. Poulsen and K. Mølmer, Phys. Rev. A **65**, 033613 (2002).

[53] A. Peters, K. Chung, and S. Chu, Nature (London) **400**, 849

(1999).

[54] D. Harber, H. Lewandowski, J. McGuirk, and E. Cornell, Phys. Rev. A **66**, 053616 (2002).

[55] S. Kokkelmans (private communication).

[56] A. Barone and G. Paterno, *Physics and Application of the Jo-*

sephson Effect (Wiley Interscience, New York, 1982).

[57] A. Leggett and F. Sols, Found. Phys. **21**, 353 (1991).

[58] E. Goldobin, K. Vogel, O. Crasser, R. Walser, W. P. Schleich, D. Koelle, and R. Kleiner, Phys. Rev. B **72**, 054527 (2005).

[59] P. Braun, Rev. Mod. Phys. **65**, 115 (1993).